

A Stable Electroactive Monolayer Composed of Soluble Single-Walled Carbon Nanotubes on ITO

Qiguan Wang[1] **and Hiroshi Moriyama***[1,2]

[1]Research Center for Materials with Integrated Properties, Toho University, 2-2-1 Miyama, Funabashi 274-8510

[2]Department of Chemistry, Toho University, 2-2-1 Miyama, Funabashi 274-8510

Received December 22, 2008; E-mail: moriyama@chem.sci.toho-u.ac.jp

Self-assembled monolayers (SAMs) of single-walled carbon nanotubes (SWNTs) covalently attached to a (3-aminopropyl)trimethoxysilane-modified ITO surface (SAM–ITO) were prepared by the coupling reaction of the amine groups with the carboxyl groups from the soluble SWNTs, which were safely obtained via a two-step process assisted by microwave irradiation. The surface composition of the SAM–ITO was examined using X-ray photoelectron spectroscopy. The cyclic voltammetry (CV) behavior of the SAM–ITO in an organic system showed a higher capacitor charging current, which indicated the presence of a tethered SWNT monolayer. However, the CV behavior of the SAM–ITO in acidic aqueous solutions showed unexpected oxidation signals because of redox reactions involving the defects and sidewalls of soluble functionalized SWNTs. To make the CVs of the resulting SWNT monolayers more stable in acidic aqueous solutions, a conductive oligomer of tetramer aniline was additionally incorporated onto the residual carboxyl groups on the SWNTs. The UV–vis spectrum showed that the SWNT monolayer was successfully endcapped by the conductive oligomer, and atomic force microscopy images showed that the SWNTs from the self-assembled monolayer were thickened and the SWNT surfaces were roughened. The CV data showed a single reversible redox couple, which indicated a more stable state.

Carbon nanotubes have unique structural characteristics that lead to many fascinating properties and potential applications in chemistry, biology, and materials science.[1–3] In particular, the high conductivity and transmittance values facilitate electron transfer to an electrode, and make carbon nanotubes very attractive for photosensors, field emission devices, and optoelectronic devices.[4–6] However, their inherent insolubility in organic solvents and their incompatibility with chemical and biological systems have delayed these applications. To improve the solubility of carbon nanotubes, two possible approaches have been proposed, involving noncovalent and covalent functionalization of the carbon nanotubes. In the noncovalent functionalization case, it is well established that single-walled carbon nanotubes (SWNTs) can be dispersed in common organic solvents via π-stacking interactions with a wide range of molecular species ranging from synthetic polymers[7–10] to organic dyes.[11–14] In the chemical functionalization case, it is reported that SWNTs are more easily solvated by the surface tails of the functional groups, particularly in the case of attached polymers.[15] Compared with those sidewall functionalizations using fluorine,[16] aryl diazonium salts,[17] azomethine ylides,[18] nitrenes,[19] carbenes,[20] Bingel reaction,[21] and organic radicals,[22,23] the functionalization of SWNTs through the oxidation route that leads to shortened nanotubes bearing carboxylic acid groups is a much simpler method and has been more explored.[24] Using this method, soluble SWNTs in a 1:1 H_2SO_4/HNO_3 (v/v) mixed solution were recently obtained using microwave radiation at a pressure of 1.4 MPa.[25] The resulting water–SWNT solution was a true solution, and the particle size was determined to be below 3 nm from laser light-scattering particle-size measurements. However, another method, such as the formation of functionalized SWNTs at lower pressure, for example at ambient pressure, is required from considerations of process safety and instrument simplicity.

In recent years, studies on self-assembled monolayers (SAMs) fabricated through functionalized SWNT molecules have progressed, and have attracted much attention, not only from the viewpoint of fundamental research but also as regards applications in device technology. Various methods such as drop-drying from solvent,[26,27] airbrushing,[28] and Langmuir–Blodgett deposition[29] have been used for the fabrication of SWNT thin films. However, the physical connection between SAMs and the substrates is a barrier in forming a stable device in comparison with chemical attachment. Although several reports have addressed the SWNT SAMs covalently linked with substrates,[30,31] the utilization of insoluble functionalized SWNTs instead of soluble SWNTs has some limitations in terms of controlling the film uniformity and production efficiency. Here, a method in which an SWNT layer is covalently attached onto an ITO is shown by employing soluble SWNTs, which were safely obtained via a two-step process assisted by microwave irradiation. Afterwards, the electrochemical stability of the SWNT layer was examined (Scheme 1).

Experimental

Chemicals and Instrumentation. The SWNTs, prepared using a high-pressure carbon monoxide (HiPco) chemical vapor deposition process, were obtained from Carbon Nanotechnologies Inc. (CNI, Texas, USA). The (3-aminopropyl)trimethoxysilane (APTMS) used was purchased from TCI (Japan). The 1,3-

Published on the web June 12, 2009; doi:10.1246/bcsj.82.743

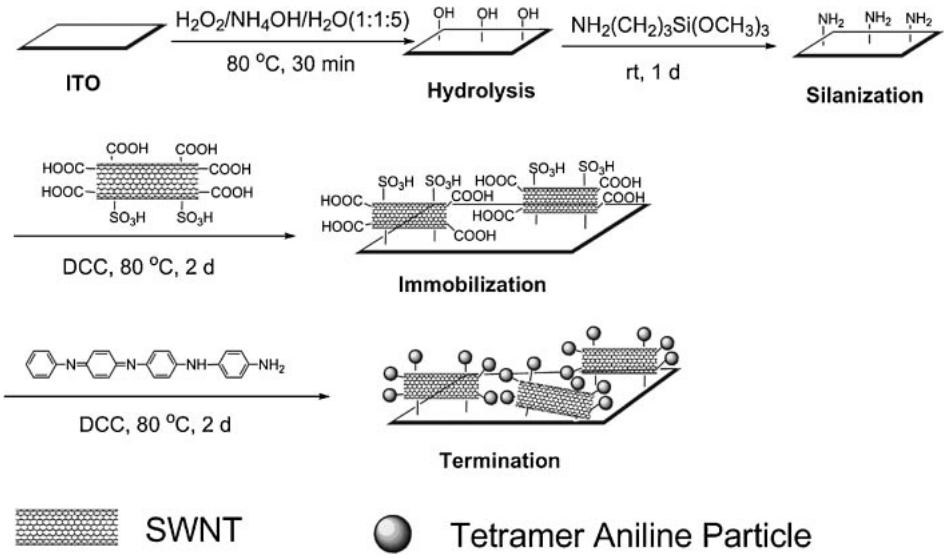

Scheme 1. Schematic illustration of the preparation route for attaching a functionalized SWNT layer onto an ITO endcapped by a tetramer aniline group.

dicyclohexylcarbodiimide (DCC) and anhydrous hydrazine were purchased from Wako (Japan). The *N*-phenyl-1,4-phenylenediamine used was obtained from Sigma-Aldrich (USA). All other chemicals used were of analytical grade and were purchased from Sigma-Aldrich and used without further purification. The microwave system used (National NE710G, Japan) could be programmed to operate at different power levels and time periods.

Preparation of Soluble Functionalized SWNTs with Terminal Carboxylic Acid Groups. It has been reported that SWNTs can be purified and slightly shortened in an H_2O_2 solution under microwave irradiation before subsequent functionalization.[32] Stimulated by this idea, soluble functionalized SWNTs were prepared in two steps assisted by a microwave oven, where the microwave power was set to 350 W. Compared with the preparation under higher pressure,[25] the two-step approach allowed for safer and easier operation. As a typical example, 20 mg of the as-received SWNTs were treated with 20 mL of concentrated H_2O_2 solution for a period of 60 s in the microwave oven in a Teflon reaction chamber with the cap unscrewed for safety reasons. The boiled solution was then allowed to cool to room temperature and was filtered using a 0.1 μm polycarbonate membrane and then rinsed with deionized (DI) water. After drying for a period of 3 h at 100 °C in a vacuum oven, the carbon nanotubes were added to 20 mL of a 1:1 v/v mixture of aqueous 70% nitric acid and 97% sulfuric acid solutions and microwave irradiated for a period of 5 min (The acid mixture and the concentrated H_2O_2 solution are highly corrosive, and therefore extreme care had to be exercised during handling.). For safety reasons, the Teflon reaction chamber was loosely capped when placed in the microwave oven until cooled to room temperature after addition of the acid mixture. The final mixture was then diluted with DI water and transferred to a dialysis bag with a nominal molecular weight cutoff of 12000–14000. The bag was soaked in DI water in a beaker. The DI water was continually refreshed until the pH of the filtrate in the bag reached pH 7. The filtrate was then removed and concentrated in a vacuum evaporator. The black functionalized SWNT residue obtained from the evaporator was additionally dried overnight at 60 °C in a vacuum oven and used for the subsequent immobilization experiments on ITO glass.

Preparation of Tetramer Aniline Oligomer Endcapped with Amine Groups. Following the Zhang et al. method,[33] tetramer aniline with a terminated amine group at one end in the emeraldine oxidation state was prepared by the suspension reaction of *N*-phenyl-1,4-phenylenediamine with ferric chloride hexahydrate. The obtained emeraldine oligomer was reduced to the leucoemeraldine oxidation state using anhydrous hydrazine in ethanol and then recrystallized from ethanol. The resulting tetramer aniline in the leucoemeraldine oxidation state was characterized using FT-IR, UV–vis, and NMR. Because of its excellent stability and high conductivity, the tetramer aniline in the emeraldine oxidation state was used to form a conductive conjugate with functionalized SWNTs in the next step.

Preparation of SAM of APTMS and Immobilization of SWNTs. The ITO plates ($20 \times 20 \times 1.1\,mm^3$, sheet resistance = $10\,\Omega\,sq^{-1}$, E. H. C. Co., Ltd.) were cut into $5 \times 20\,mm^2$ coupons and ultrasonically precleaned with acetone, ethanol, and a copious amount of DI water. To obtain uniformly distributed OH groups on the ITO surface, the ITO glass samples were immersed in a solution of $H_2O_2/NH_4OH/H_2O$ (1:1:5, v/v/v) for a period of 30 min at 80 °C for hydrolysis, after which they were rinsed thoroughly with DI water and dried. The hydrolyzed ITO plates were immersed in a 1% (v/v) solution of APTMS in toluene overnight at room temperature for silanization. After the coupling reaction, the ITO glass was rinsed with toluene and water to remove the physically adsorbed silanes from the surface. The modified ITO glass was then dynamically dried under vacuum. SWNT immobilization occurred via a coupling reaction between the amino group of the silane and the DCC-activated carboxyl groups on the surface of the SWNT. For immobilization, 5.0 mg of a functionalized SWNT was ultrasonically dispersed in 30 mL of DMF containing 4.0 mg of DCC, resulting in a true SWNT solution. The SWNT was covalently attached to APTMS SAM on the ITO surface immersed in the SWNT solution at 80 °C for a period of 48 h (Scheme 1). The ITO sample was then removed and thoroughly rinsed using DMF, acetone, and water to remove any unbound SWNT and DCC and dried at room temperature. To terminate the residual carboxyl groups at the end of the SWNTs on ITO, the dried ITO samples were immersed in 10 mL of DMF

containing 30 mg of tetramer aniline terminated by amine groups and 6.0 mg of DCC, then kept for 48 h at 80 °C. The ITO was finally washed thoroughly using DMF and acetone and dried.

Measurements. The soluble functionalized SWNTs were analyzed using an FT-IR spectrometer (JASCO FT/IR-4100A, Japan) employing the KBr disk method. The characteristic absorbance measurements of the tetramer aniline coupled on the ITO plate were carried out using a UV–vis spectrophotometer (JASCO UV-550, Japan). The ^{1}H and ^{13}C NMR spectra of the tetramer aniline with a terminated amine group were characterized using a Bruker Avance II 400 MHz spectrometer. Cyclic voltammetry of the samples was performed at room temperature using a BAS 100B analytical system from Tokyo, Japan, with an ALS/CHI600A electrochemical analyzer (CH Instruments Inc., Austin, USA), in 15 mL of acetonitrile solution ($Ag/AgNO_3$ in a 0.1 M ($1\,M = 1\,mol\,dm^{-3}$) tetrabutylammonium perchlorate (TBAP)/CH_3CN solution was used as the reference electrode), containing 0.1 M TBAP as a supporting electrolyte, or in 15 mL of 1.0 M H_2SO_4 aqueous solution (Ag/AgCl in a saturated 3 M NaCl solution was used as the reference electrode). A SAM–ITO plate was used as the working electrode, and a Pt wire ($\phi = 0.3$ mm) was used as the counter electrode. The voltage in most of the experiments was scanned at a rate of $0.05\,V\,s^{-1}$, starting at the most positive (oxidizing) potential. The morphology of the ITO surfaces was examined using a Shimadzu SPM-9600 atomic force microscope. X-ray photoelectron spectroscopy (XPS) was used to measure the surface composition of the ITO samples. Measurements were performed using a JEOL JPS-90SX spectrometer equipped with a monochromatic Mg Kα X-ray source (1253.6 eV). The instrument was operated with an analyzer chamber pressure maintained below 10^{-9} Torr. The binding energy was referenced to the C 1s signal of the alkyl chains or alkyl contaminants at 284.6 eV.

Results and Discussion

FT-IR of Soluble Functionalized SWNTs. The FT-IR spectra of the soluble functionalized SWNTs were obtained to determine the structure of the chemical groups formed on the nanotube sidewalls and tube ends (Figure 1). The spectrum of the SWNTs that were purified and shortened by microwave H_2O_2 treatment (blue curve) is similar to that for pristine SWNT (black curve), which showed that the functionalization was limited, and the SWNT C=C graphitic stretching mode at 1570 cm^{-1} was less defined. The broad peak at 3430 cm^{-1} in pristine SWNT and shortened SWNT, and the peak at 1636 cm^{-1} observed in all of the spectra, could be due to traces of water in making the KBr pellets.[34,35] After further microwave irradiation with acid mixture, a typical FT-IR spectrum (red curve) showed several strong infrared peaks compared with that of the H_2O_2-treated SWNTs. The peak occurring at 1730 cm^{-1} was assigned to the C=O stretching mode of the –COOH groups from the SWNT backbone, and the intense broad peak centered at 3402 cm^{-1} was assigned to the –OH stretching mode of the –COOH group and the –COH group. The intense broad peak centered at 1630 cm^{-1} from 1500 to 1680 cm^{-1} resulted from the overlapping features of water impurity in the KBr pellet and the SWNT C=C graphitic stretching mode, which is more infrared active because of extensive sidewall functionalization. The weaker peak observed at 1390 cm^{-1} was attributed to the asymmetric SO_2 stretching mode of the acid sulfonate ($–SO_2OH$) group, accompanied by the lower wavenumber peak at 1132 cm^{-1} assigned to the SO_2 symmetric stretching mode. The FT-IR spectrum is consistent with that reported earlier,[25] which showed that most of the functionalized carbon atoms on the SWNT backbone were carboxylated, with the remainder being sulfonated. The extensive carboxylation and acid sulfonation on the SWNTs induced the functionalized SWNTs to form a true solution in polar solvents because of the formation of an SWNT polyelectrolyte salt via ionic dissociation.

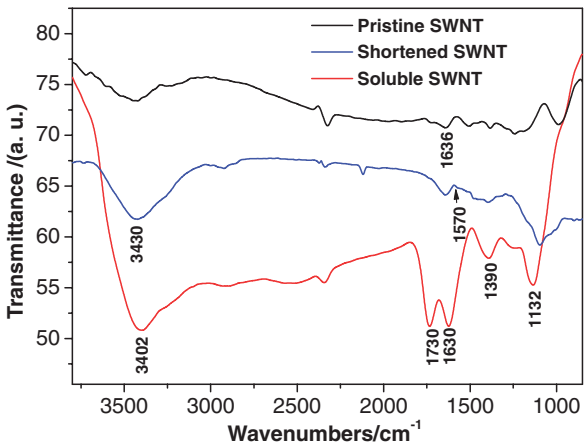

Figure 1. FT-IR spectra of pristine SWNT (black curve), H_2O_2-treated SWNT (shortened SWNT, blue curve), and soluble functionalized SWNT (red curve).

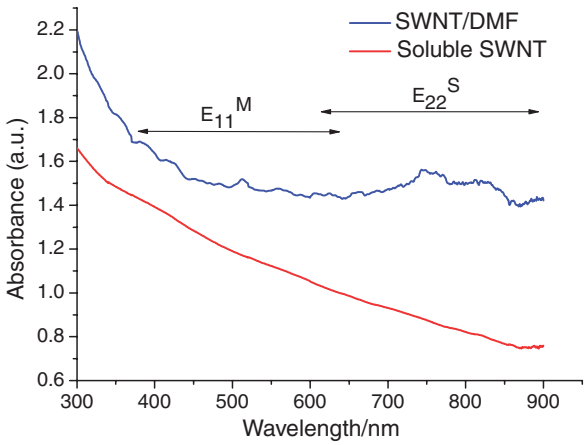

Figure 2. UV–vis spectra of (a) pristine SWNTs in DMF ($0.05\,mg\,mL^{-1}$) and (b) functionalized SWNTs in aqueous solution ($1.0\,mg\,mL^{-1}$).

Electronic and Optical Properties of Soluble Functionalized SWNTs. Because the electronic and optical properties of carbon nanotubes vary substantially with structure functionalizations, UV–vis spectra of a suspension of pristine SWNT in DMF and aqueous dispersions of soluble SWNTs were compared, as shown in Figure 2. The UV–vis spectrum of pristine SWNTs (blue curve) clearly demonstrates the van Hove singularities attributed to the band gap transitions in metallic (E_{11}^{M}) and semiconducting (E_{22}^{S}) nanotubes because of the electronic structure of the nanotubes.[36,37] The width of these features is due to the overlap of features from tubes of different

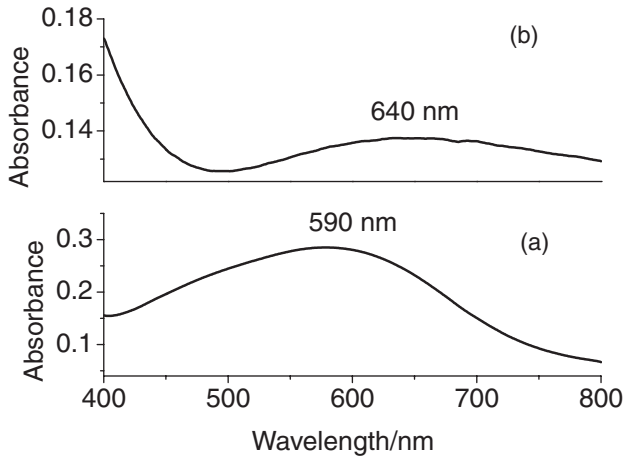

Figure 3. UV–vis spectra of tetramer aniline emeraldine in (a) DMF and (b) SAM–ITO endcapped by tetramer aniline groups.

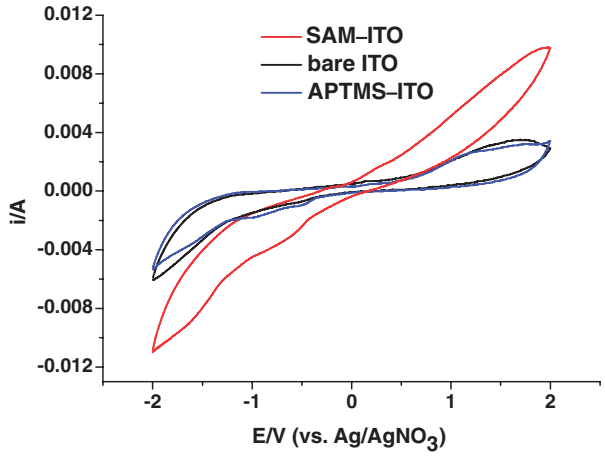

Figure 4. CV traces of bare ITO, APTMS-modified ITO (APTMS–ITO), and SWNT-functionalized ITO (SAM–ITO) in CH_3CN with 0.1 M TBAP as the supporting electrolyte. Scan rate: 0.05 V s^{-1}.

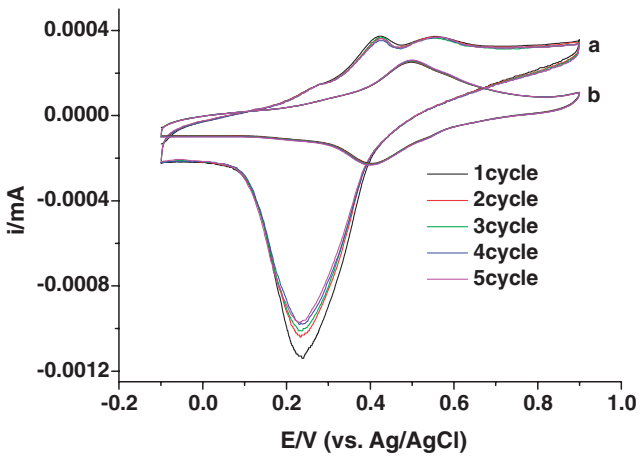

Figure 5. CV traces of (a) SAM–ITO and (b) SAM–ITO endcapped by tetramer aniline groups in an aqueous 1.0 M H_2SO_4 solution. Scan rate: 0.05 V s^{-1}.

diameters and chiral indices. After two-step microwave irradiation, these transitions are no longer visible for soluble functionalized SWNTs (red curve), and the spectrum is essentially featureless. The loss of structure in the absorption spectrum is indicative of significant electronic perturbation of the SWNTs and disruption of the extended π network.[38] This effect is consistent with covalent functionalization from the FT-IR result, rather than simple adsorption to the nanotube walls or end caps.

UV–Vis of SAM–ITO. Figure 3 shows the UV–vis absorption spectrum of SAM–ITO glass with endcapped tetramer aniline groups, where the characteristic localized polaron absorption peak at 640 nm was observed (Figure 3b), which showed the successful attachment of tetramer aniline molecules to the surface of the SWNTs. Interestingly, a red shift of about 50 nm was observed compared with the spectrum of tetramer aniline in the emeraldine oxidation state (590 nm),[33] as shown in Figure 3a for the localized polaron absorption band, which could be induced by π–π interactions across the SWNT and the tetramer aniline molecule.

Cyclic Voltammetry (CV) Analysis. To confirm the immobilization of the functionalized SWNTs with amine groups on the modified ITO glass by DCC chemistry, CV measurements were carried out using the SAM–ITO as the working electrode in a 0.1 M TBAP/acetonitrile solution. A higher capacitor charging current in the SAM–ITO than in the bare ITO plates was expected, as shown by the curves in Figure 4, which is attributed to the presence of SWNTs, resulting in an increase in the active electrochemical components.

To evaluate the stability in water of the water-soluble SWNT layer, the SAM–ITO electrode was successively scanned for five cycles from −0.1 to 0.9 V at a rate of 0.05 V s^{-1} in a 1.0 M H_2SO_4 aqueous solution. Surprisingly, the CV data of the SAM–ITO electrodes demonstrated that two oxidation peaks occurred at 0.42 and 0.56 V, although only one reduction peak occurred at ca. 0.24 V (Figure 5a). Additionally, the current peaks were gradually decreased with the increase of CV cycles, which showed a lower stability than in an organic TBAP/acetonitrile solution. Taking into account the defect structures of oxidized aromatic rings on the SWNTs, these peaks below 0.6 V can be assigned to the redox reactions of oxidative sidewalls through an electron-transfer quinone/hydroquinone mechanism (0.42 V) and a possible mechanism for the oxidation/reduction of carboxylic acid/anhydride (0.56 V) in acidic aqueous systems (Scheme 2).[39] Similar electrochemical reactions in aqueous solution, associated with surface oxygen complexes and increasing defect densities of the carbon nanotubes, have been reported and assigned previously.[40] However, the CV data recorded for tetramer aniline endcapped SAM–ITO (Figure 5b) showed two reversible redox couples occurring at 0.50 and 0.40 V under the same conditions, which were assigned to the oxidation and reduction of the tetramer aniline between the leucoemeraldine and emeraldine oxidation states.[41] Moreover, this was very reproducible, indicating that the stability of the SAM–ITO was improved after being endcapped by the tetramer aniline molecules. We concluded that the introduction of endcapped tetramer aniline groups on the SAM–ITO decreases the number of unstable defects, and the sidewalls of the soluble functionalized SWNT are protected via π–π interactions, together with the doping effect between

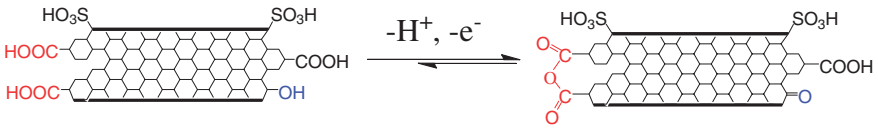

Scheme 2. Schematic illustration of the proposed mechanism for the redox processes corresponding to the CV peaks of the soluble functionalized SWNTs.

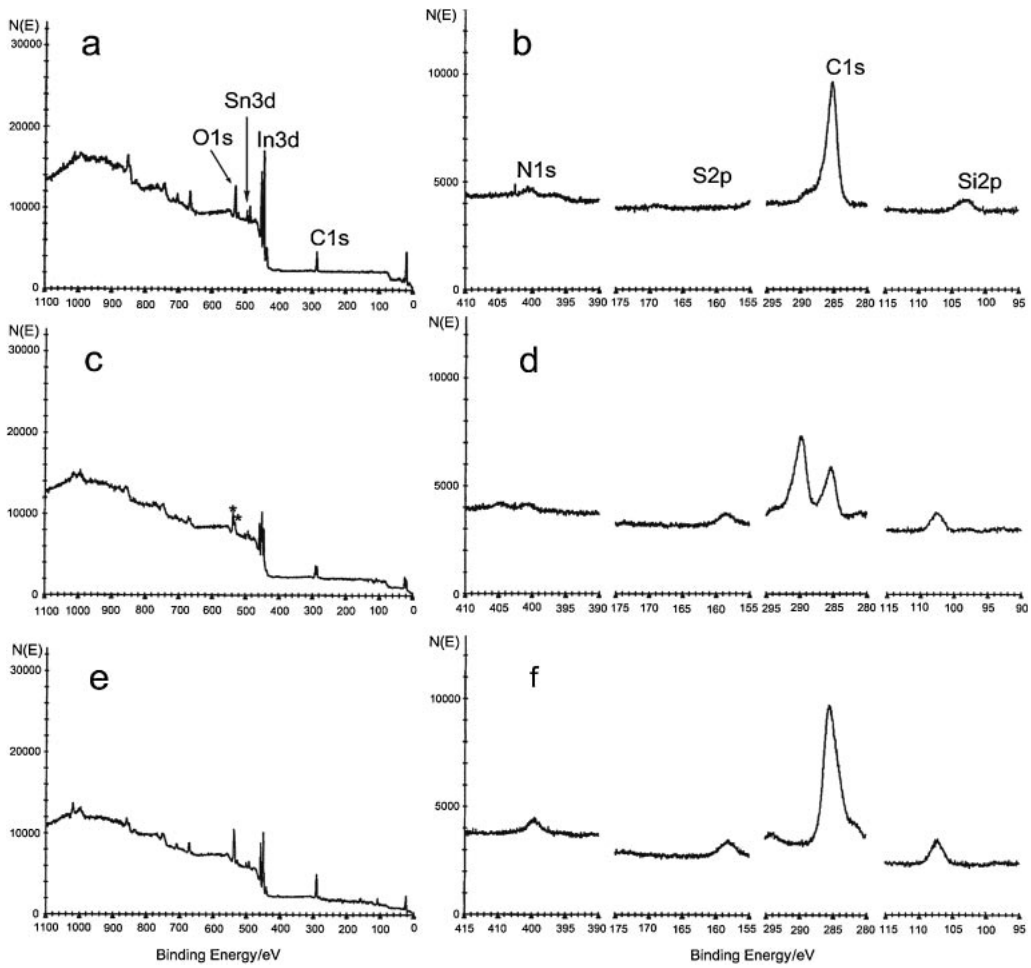

Figure 6. The XPS wide-scan spectra of (a) pristine ITO, (c) SAM–ITO, (e) tetramer aniline-terminated SAM–ITO surface, and (b), (d), and (f) their corresponding high-resolution N 1s, S 2p, C 1s, and Si 2p spectra, respectively.

the residual sulfonic groups on the SWNT surface and the tetramer aniline backbone. This results in the higher stability of the SWNT on oxidation in the CV scan.

The surface coverage can be calculated by integration of the reduction peak current.[42] It was calculated to be 4.1×10^{-12} mol cm^{-2} for the SAM–ITO and 3.2×10^{-12} mol cm^{-2} for the SAM–ITO terminated by tetramer aniline groups, which are about two orders of magnitude lower than that for the general monolayer (10^{-10} mol cm^{-2}) of small functional molecules because of the poor reaction efficiency resulting from the large geometry of SWNTs. It should be noted that the surface coverage of SAM–ITO could be further improved by repeating this amidation coupling via a linking reagent with double amine tails.

XPS and Atomic Force Microscopy (AFM) Images. In general, electron spectroscopy techniques used for chemical analysis, such as XPS, provide qualitative and quantitative information about the elemental composition of matter, which is particularly useful for the characterization of composite surfaces. The corresponding near-surface composition of the functionalized SWNTs deposited on ITO plates was determined using XPS, as shown in Figure 6. In addition to the intense and sharp features of the In 3d, Sn 3d, and O 1s peaks, the spectrum of the bare ITO plate exhibited weak C 1s and Si 2p peaks, which correspond to minor surface carbon contamination and the silicon from the glass, respectively (Figures 6a and 6b).[43,44] After attachment of the soluble functionalized SWNT, the peak intensity of the In 3d, Sn 3d, and O 1s peaks decreased, and the Si 2p peaks increased, because of the linked APTMS agent between the ITO layer and the functionalized SWNT (Figures 6c and 6d). In addition, the observed S 2p feature showed the presence of acid sulfonate (–SO_2OH)

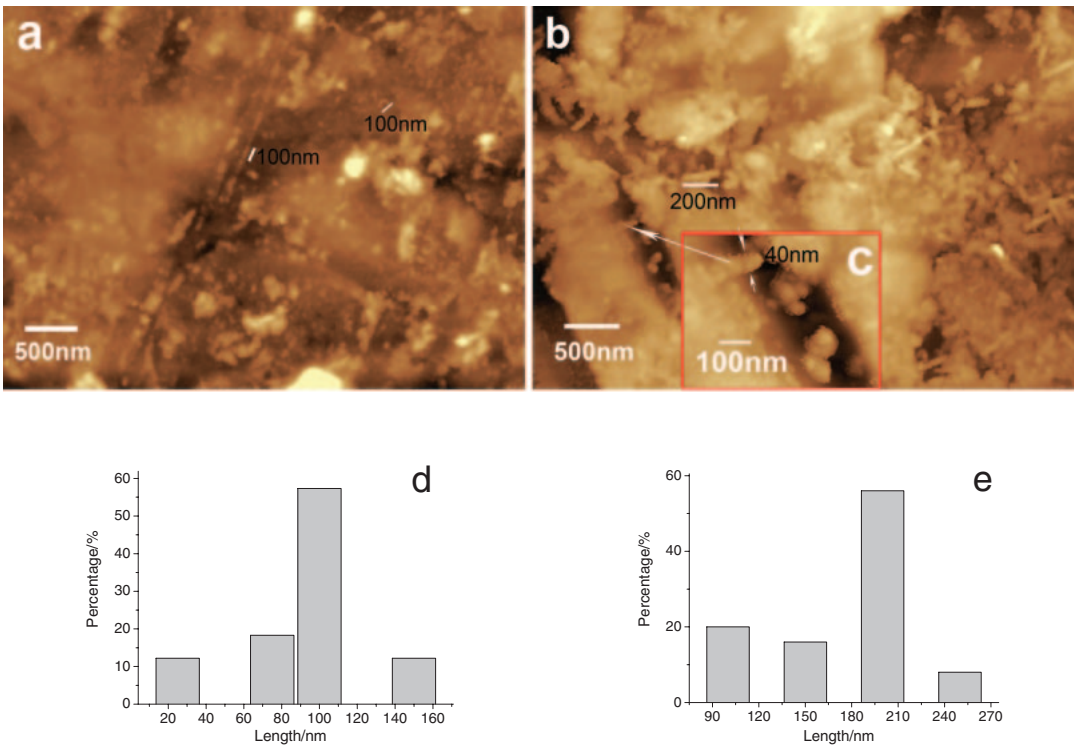

Figure 7. Tapping mode AFM images of (a) SAM–ITO and (b) tetramer aniline-terminated SAM–ITO surface. Insert (c) shows the high-resolution image of (b). (d) and (e) are the length histograms of SWNTs from the AFM data of (a) and (b), respectively.

groups on the functionalized SWNTs, which is consistent with the FT-IR data discussed above. Aside from the C–C/C–H peak at 285.3 eV, an additional photoemission representing the higher binding energy bands indicated the presence of carbon atoms bonded to other functional groups. The binding energy peak occurring at 290 eV was attributed to C=O and O–C=O groups from the functionalized SWNTs. The two-peak feature of O 1s peaks (denoted by asterisks in Figure 6c) shown in the wide-scan spectra compared with that of the bare ITO plate also offers evidence for different chemically bonded states that correspond to COOH groups on the functionalized SWNT surface. However, after endcapping the residual carboxylic acid groups by the tetramer aniline terminated by amine groups, the intensity of the C 1s and O 1s features in the higher binding energy bands was significantly decreased to form a shoulder peak, as shown in Figures 6e and 6f. In addition, from the corresponding peak areas, the relative atomic content of the C 1s and N 1s peaks was enhanced compared with that of the In 3d or Sn 3d peaks. This is reasonable, considering that the enriched particle assembled by end-terminated tetramer aniline molecules tightly covered the sidewalls of the soluble functionalized SWNT via π–π interactions, where only the photoemissions of the C 1s and N 1s peaks assigned to the tetramer aniline backbone were detected. This results in an increase in the N 1s and C 1s peaks in the lower binding energy bands, and a decrease in the C 1s and O 1s peaks in the higher binding energy bands.

The surface morphology of SAM–ITO and tetramer aniline-terminated ITO plates was examined using AFM. From Figure 7a, the SAM–ITO plate showed a monolayer with tube-like particle topography, implying the successful incorporation of functionalized SWNTs onto the ITO surface. The average length of the functionalized SWNTs is around 100 nm (Figure 7d), demonstrating that extensive shortening during microwave treatment has occurred. Their average diameter is around 20 nm, implying that most of the functionalized SWNTs on the ITO surface were significantly debundled under the chemical bonding. The morphology of the obtained SWNT layer was significantly changed after being endcapped using tetramer aniline groups (Figure 7b), which showed a rougher SWNT surface compared with that of SAM–ITO (see arrow label in Figure 7c). From the AFM image shown in Figure 7b, the average length of the tetramer aniline-terminated SWNTs is around 200 nm (Figure 7e) with an average diameter of around 40 nm, which showed a significant increase compared with that of the pure SWNT layer, because of the presence of a tetramer aniline particle layer linked with functionalized SWNTs by CO–NH bonds. As discussed above, the conjugate layer, assembled by the end-terminated tetramer aniline molecules, tightly covered the sidewalls of the soluble functionalized SWNTs via covalent bonding and π–π interactions, together with the doping effect between tetramer aniline and the sulfonic groups on the SWNT surface, which made the SWNT layer more stable in the CV scans in acidic aqueous solutions.

Conclusion

Soluble SWNTs were safely prepared by the assistance of microwaves via a two-step method at ambient pressure, in contrast to previous methods. The chemically anchored SWNT SAM on an ITO plate functionalized by APTMS was then

successfully fabricated from the DCC coupling of the carboxyl groups on the surface of the SWNTs with the amine groups on the surface of the ITO. These showed a higher capacitor charging current using a CV instrument. However, the SAM–ITO was easily oxidized in acidic aqueous solutions because of the presence of defects susceptible to oxygen, including the residual carboxyl groups on the SWNT wall, together with the considerable quantity of sulfonic groups. In addition, when endcapped by a conjugated compound, such as a tetramer aniline, the SAM–ITO showed more stable CV behavior in acidic aqueous solutions, which exhibited two reversible redox couples characteristic of the conductive state of the tetramer aniline under the same conditions. AFM images showed that the diameter of the SWNTs on ITO was increased and the surface was roughened after being endcapped by a tetramer aniline group. Both the doping of tetramer aniline with the sulfonic groups on the SWNT surface and the tight protection by the π–π interaction between the tetramer aniline groups and the SWNT walls probably made the SAM–ITO more stable, as seen in the CV scans, and as demonstrated by UV and XPS data. It is expected that this stable electroactive SWNT layer will find a wealth of applications in nanocomposite architectures.

We are grateful to the Sumitomo Corporation for donating the HiPco SWNTs from CNI (Texas, USA). We thank Mr. R. Osada, Chiba Institute of Technology, Japan, for measuring the XPS and Mr. A. Kogure, Shimadzu Corporation, Japan, for measuring the AFM.

References

1 S. Iijima, T. Ichihashi, *Nature* **1993**, *363*, 603.
2 H. J. Dai, *Acc. Chem. Res.* **2002**, *35*, 1035.
3 D. Tasis, N. Tagmatarchis, A. Bianco, M. Prato, *Chem. Rev.* **2006**, *106*, 1105.
4 M. W. Rowell, M. A. Topinka, M. D. McGehee, H.-J. Prall, G. Dennler, N. S. Sariciftci, L. Hu, G. Gruner, *Appl. Phys. Lett.* **2006**, *88*, 233506.
5 J. N. Heo, J. H. Lee, T. W. Jeong, C. S. Lee, W. S. Kim, Y. W. Jin, J. M. Kim, S. G. Yu, W. K. Yi, S. H. Park, T. S. Oh, J. B. Yoo, *Appl. Phys. Lett.* **2005**, *87*, 114105.
6 D. B. Mawhinney, V. Naumenko, A. Kuznetsova, J. T. Yates, Jr., J. Liu, R. E. Smalley, *J. Am. Chem. Soc.* **2000**, *122*, 2383.
7 M. J. O'Connell, P. Boul, L. M. Ericson, C. Huffman, Y. Wang, E. Haroz, C. Kuper, J. Tour, K. D. Ausman, R. E. Smalley, *Chem. Phys. Lett.* **2001**, *342*, 265.
8 A. Star, J. F. Stoddart, D. Steuerman, M. Diehl, A. Boukai, E. W. Wong, X. Yang, S.-W. Chung, H. Choi, J. R. Heath, *Angew. Chem., Int. Ed.* **2001**, *40*, 1721.
9 J. Chen, H. Liu, W. A. Weimer, M. D. Halls, D. H. Waldeck, G. C. Walker, *J. Am. Chem. Soc.* **2002**, *124*, 9034.
10 D. W. Steuerman, A. Star, R. Narizzano, H. Choi, R. S. Ries, C. Nicolini, J. F. Stoddart, J. R. Heath, *J. Phys. Chem. B* **2002**, *106*, 3124.
11 H. Murakami, T. Nomura, N. Nakashima, *Chem. Phys. Lett.* **2003**, *378*, 481.
12 S. Bhattacharyya, E. Kymakis, G. A. J. Amaratunga, *Chem. Mater.* **2004**, *16*, 4819.
13 C. G. Hu, Z. L. Chen, A. G. Shen, X. C. Shen, J. Li, S. S. Hu, *Carbon* **2006**, *44*, 428.
14 C.-H. Liu, J.-J. Li, H.-L. Zhang, B.-R. Li, Y. Guo, *Colloids Surf., A* **2008**, *313–314*, 9.
15 C.-Y. Hong, Y.-Z. You, D.-C. Wu, Y. Liu, C.-Y. Pan, *Macromolecules* **2005**, *38*, 2606.
16 E. T. Mickelson, C. B. Huffman, A. G. Rinzler, R. E. Smalley, R. H. Hauge, J. L. Margrave, *Chem. Phys. Lett.* **1998**, *296*, 188.
17 J. L. Bahr, J. Yang, D. V. Kosynkin, M. J. Bronikowski, R. E. Smalley, J. M. Tour, *J. Am. Chem. Soc.* **2001**, *123*, 6536.
18 D. Pantarotto, C. D. Partidos, R. Graff, J. Hoebeke, J.-P. Briand, M. Prato, A. Bianco, *J. Am. Chem. Soc.* **2003**, *125*, 6160.
19 M. Holzinger, J. Abraham, P. Whelan, R. Graupner, L. Ley, F. Hennrich, M. Kappes, A. Hirsch, *J. Am. Chem. Soc.* **2003**, *125*, 8566.
20 H. Hu, B. Zhao, M. A. Hamon, K. Kamaras, M. E. Itkis, R. C. Haddon, *J. Am. Chem. Soc.* **2003**, *125*, 14893.
21 K. S. Coleman, S. R. Bailey, S. Fogden, M. L. H. Green, *J. Am. Chem. Soc.* **2003**, *125*, 8722.
22 H. Peng, P. Reverdy, V. N. Khabashesku, J. L. Margrave, *Chem. Commun.* **2003**, 362.
23 Y. Ying, R. K. Saini, F. Liang, A. K. Sadana, W. E. Billups, *Org. Lett.* **2003**, *5*, 1471.
24 J. Chen, M. A. Hamon, H. Hu, Y. Chen, A. M. Rao, P. C. Eklund, R. C. Haddon, *Science* **1998**, *282*, 95.
25 Y. B. Wang, Z. Iqbal, S. Mitra, *J. Am. Chem. Soc.* **2006**, *128*, 95.
26 T. V. Sreekumar, T. Liu, S. Kumar, L. M. Ericson, R. H. Hauge, R. E. Smalley, *Chem. Mater.* **2003**, *15*, 175.
27 W. Lee, J. Lee, S.-H. Lee, J. Chang, W. Yi, S.-H. Han, *J. Phys. Chem. C* **2007**, *111*, 9110.
28 M. Kaempgen, U. Dettlaff, S. Roth, *Synth. Met.* **2003**, *135–136*, 755.
29 Y. Kim, N. Minami, W. Zhu, S. Kazaoui, R. Azumi, M. Matsumoto, *Jpn. J. Appl. Phys.* **2003**, *42*, 7629.
30 P. Diao, Z. F. Liu, B. Wu, X. L. Nan, J. Zhang, Z. Wei, *ChemPhysChem* **2002**, *3*, 898.
31 Y. J. Zhang, J. Li, Y. F. Shen, M. J. Wang, J. H. Li, *J. Phys. Chem. B* **2004**, *108*, 15343.
32 S. Y. Hong, G. Tobias, B. Ballesteros, F. E. Oualid, J. C. Errey, K. J. Doores, A. I. Kirkland, P. D. Nellist, M. L. H. Green, B. G. Davis, *J. Am. Chem. Soc.* **2007**, *129*, 10966.
33 W. J. Zhang, J. Feng, A. G. MacDiarmid, A. J. Epstein, *Synth. Met.* **1997**, *84*, 119.
34 Y. B. Wang, Z. Iqbal, S. Mitra, *Carbon* **2005**, *43*, 1015.
35 Y. B. Wang, Z. Iqbal, S. Mitra, *Carbon* **2006**, *44*, 2804.
36 Y. Miyauchi, S. Chiashi, Y. Murakami, Y. Hayashida, S. Maruyama, *Chem. Phys. Lett.* **2004**, *387*, 198.
37 Y. Noguchi, T. Fujigaya, Y. Niidome, N. Nakashima, *Chem.—Eur. J.* **2008**, *14*, 5966.
38 B. A. Kakade, V. K. Pillai, *Appl. Surf. Sci.* **2008**, *254*, 4936.
39 M. J. Bleda-Martínez, D. Lozano-Castelló, E. Morallón, D. Cazorla-Amorós, A. Linares-Solano, *Carbon* **2006**, *44*, 2642.
40 J. G. Zhou, C. Booker, R. Y. Li, X. T. Zhou, T.-K. Sham, X. L. Sun, Z. F. Ding, *J. Am. Chem. Soc.* **2007**, *129*, 744.
41 L. Chen, Y. H. Yu, H. P. Mao, X. F. Lu, W. J. Zhang, Y. Wei, *Mater. Lett.* **2005**, *59*, 2446.
42 P. Bertoncello, I. Ciani, F. Li, P. R. Unwin, *Langmuir* **2006**, *22*, 10380.
43 S. Li, E. T. Kang, Z. H. Ma, K. L. Tan, *Surf. Interface Anal.* **2000**, *29*, 95.
44 K. R. Kissell, K. B. Hartman, P. A. W. Van der Heide, L. J. Wilson, *J. Phys. Chem. B* **2006**, *110*, 17425.